Corrosion protection mechanisms of TiMgN hard coatings on steel

IOP Conf. Series: Materials Science and Engineering **373** (2018) 012009 doi:10.1088/1757-899X/373/1/012009

Corrosion protection mechanisms of TiMgN hard coatings on steel

A Heyn[1], T Mueller[2], M Balzer[3], H Kappl[3] and M Fenker[3]

[1] Otto-von-Guericke-University Magdeburg, Institute of Materials and Joining Technology, Magdeburg, Germany
[2] Bundesanstalt für Materialforschung und –prüfung, Division 7.6 Corrosion and Corrosion Protection, Berlin, Germany
[3] fem, Forschungsinstitut Edelmetalle + Metallchemie, Schwäbisch Gmünd, Germany

Abstract. Hard coated steel components are used in a wide application range, mostly for protective, wear resistant and decorative purposes. Despite of these coatings being regarded as relatively dense, there is always a high risk of localized corrosion when a coated low alloyed steel component encounters a surrounding high humidity atmosphere or even an aqueous medium. An approach to enhance the corrosion properties is the addition of magnesium to physical vapor deposited hard coatings, like TiN. It has been found that there is a remarkable increase in corrosion resistance in dependence of magnesium content of the TiMgN coating and its surface properties. In this work the authors will explain the underlying corrosion protection mechanisms by means of electrochemical and analytical studies. The positive impact of magnesium in the coating relates on its preferred dissolution vs. steel. This causes the potential to shift to more negative direction with respect to the steel substrate and additionally leads to a temporarily passivation of the steel due to alkalization of the surrounding electrolyte by formation of magnesium hydroxide.

1. Introduction

By using hard coatings on steel wear resistant and protective functional surfaces can be created. The most popular hard coating type “TiN” is almost anodically inert and usually gets deposited with only a few micrometers of thickness. These coatings are only corrosion protective versus the underlying steel due to their barrier functionality. Unavoidable defects in the coating, often originated during their production or in operation, can lead to localized corrosion phenomena if aqueous electrolyte (water / water vapor) reaches the unprotected steel.

An alternative approach to change the electrochemical, mechanical and visual properties of the coating is the incorporation of magnesium into a PVD hard coating such as TiN via a magnetron sputtering process. For example, hardness or oxidation resistance at higher temperatures can be changed as well as color from gold-yellowish to blue-greyish [1]. A first indication of a change of their corrosion protection properties were revealed by potential measurements in 0.8 M NaCl solution. They showed that the open circuit potentials (OCP) of TiMgN coatings deposited on glass are temporarily lower than those of steel and that the steel can be temporarily protected cathodically. The more Mg is deposited, the lower the potentials and the longer this effect will last. In [2], Fenker et al. found an improvement in the corrosion behavior of TiMgN hard coatings on high-speed steel (HSS) from about 17 at-% Mg content based on results in the salt spray test.

Based on the observations that co-deposited magnesium has a positive effect on corrosion protection properties of the TiMgN hard coatings (see Fig. 1), further research was carried out starting in 2012. The work was financially supported by the German Research Foundation (DFG) and aimed to elucidate the underlying mechanisms and further improve the layer properties [3]. In this project, TiMgN coatings with 0, 10, 20 and 35 at% Mg, respectively on polished and blasted substrates made of glass and HSS substrates, were considered.

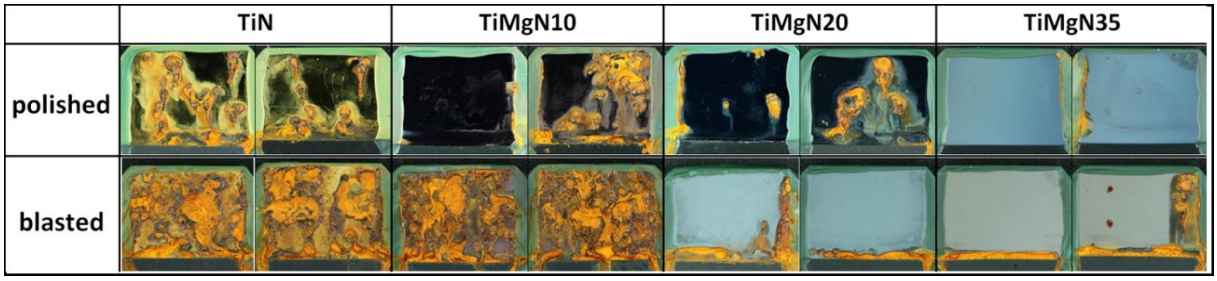

Fig. 1. Appearance of TiN and TiMgN hard coatings on HSS-substrates after 24 h NSS test

Based on OCP measurements with subsequent Mg content measurements of the NaCl-solutions, galvanic current measurements between TiMgN and steel, polarization measurements and camera-based experiments with gel pads, several underlying hypotheses for the improved corrosion protection have been established [4], e.g. the effect of the cathodic protection of the steel by preferably dissolving magnesium. However, since the TiMgN coating's OCP was found to be only temporarily more negative than steel, at least one additional mechanism had to be effective, to which the improved protection against local corrosion of the steel substrates could be attributed. A further focus was on the released Mg ions, which alkalinize the electrolyte at the interface to the exposed steel (Fe) by formation of hydroxides ($Mg(OH)_2$ and/or FeOOH), whereby the steel gets in a passive state. To demonstrate this effect, the release rates of Mg from the TiMgN hard coatings and the protection of steel in different $Mg(OH)_2$ solutions with different NaCl contents were investigated.

2. Specimen properties and experimental procedures

2.1. TiMgN fabrication and properties

Semi-circular samples of hardened low alloyed steel 100Cr6 with a diameter of 30 mm were used as substrate material for the various coatings. For corrosion tests the substrate materials were used in two surface states: corundum-blasted and polished for triggering very high and very low growth defect concentrations, respectively. These extremely opposite types of surfaces should help to understand the influence of growth defects on the corrosion behavior of the coating-substrate systems. Studies on Ti_xMg_yN systems [2] have shown that there were specific ranges of Mg content resulting in different corrosion behavior of the coatings. In scope of this work two different Mg contents (20 and 35 at-% Mg) were chosen to characterize the electrochemical behavior of TiMgN coating systems. The true Mg-concentration, measured by energy dispersive X-ray spectroscopy (EDX), was 19.9 at-% and 33.8 at-% respectively.

All coatings were deposited by reactive DC magnetron sputtering with a thickness between 2.5 and 3.0 µm in a vacuum plant Leybold L560 UV using a special magnetron arrangement. It consists of three circular 2" magnetrons (US Inc.) arranged in a triangle all facing a one-fold rotating flat substrate holder at 4.5 cm distance. Two cathodes were used for each deposition, one equipped with a Ti- (99.9 at-% purity) and one with a Mg-target (99.95 at-% purity). The desired Mg-contents of the TiMgN films were realized by adjusting the power fed to the Mg-target while keeping a constant target power for Ti. All coatings were deposited at a bias voltage U_{Bias} = -50 V and a total pressure of

p = 0.4 Pa. The basic N_2 partial pressure was p_{N_2} = 0.05 Pa and the substrate temperature was 200 °C. Prior to the depositions the substrates were plasma etched at U_{Bias} = -1000 V at p_{Ar} = 2.6 Pa with additional cathode support.

The surface of the hard coatings on polished substrate showed a columnar structure, but also common growth defects, which were characterized using "large area high resolution" (LAHR) mapping, as described by Balzer in [5]. Typical coating defects are so called hillocks of different sizes, which may have pores or crevices down to steel substrate, or be broken out, exposing the substrate to the environment at open holes of different size. On the other hand, hard coatings on blasted substrate showed a very high amount of disorder, a porous structure and a much rougher surface.

2.2. Electrochemical and analytical investigations

Samples of TiMgN with 20 and 35 at-% Mg deposited on polished and blasted 1.3505 steel were exposed to aqueous solutions with different levels of NaCl for up to 180 min and the OCP and dissolution kinetics were recorded. For this purpose, small areas of the sample surface were prepared by means of a perforated adhesive film. Then, a 3 mm in diameter measuring cell was attached thereto. The OCP was measured versus a saturated Ag/AgCl reference electrode, with a reference potential of 199 mV_{NHE}. In order to continuously determine the kinetic characteristic of the currently occurring corrosion reactions without significantly influencing the sample surface, the method of electrochemical frequency modulation (EFM) was used. In this case, a sinusoidal polarization (0.1 Hz base frequency, 0.2 and 0.5 Hz secondary frequencies) with an amplitude of 5 mV was impressed on the OCP at time-defined intervals (here every 5 min). As a result, the current polarization resistance (RP) and the simultaneously determined a/b factors (anodic and cathodic slopes) are used to obtain the instantaneous corrosion current. Details of this electrochemical methodology are described by Bosch et al. [6, 7]. The investigations were carried out with the measuring system Interface 1000 and the associated software Framework Data Acquisition from Gamry Instruments.

To investigate the release rate of magnesium, support from Max-Planck-Institute for Iron Research GmbH Düsseldorf (working group of M. Rohwerder) was accepted thankfully. There is an analytical method available, which uses a miniaturized scanning flow cell (SFC, cell diameter approx. 200 µm), that transfers the measuring electrolyte from the sample surface continuously for analysis by inductively coupled plasma mass spectrometry (ICP-MS). Thus, metal ions currently in solution (here Mg, Fe, Ti) can be analyzed with a short time shift (about 30 s). TiMgN samples with 20 and 35 at-% Mg were investigated, respectively on polished and blasted steel substrates and on glass. A 0.05 M NaCl solution was used as test electrolyte. Details of this methodology can be found in [8].

Furthermore, investigations on steel samples of 1.0535 carbon steel (C55, wet ground with P320 sandpaper) were carried out in differently concentrated $Mg(OH)_2$ solutions with different contents of NaCl. The aim was to determine the mode of action and the interaction of these electrolyte constituents on the passivity and corrosion of unalloyed steel. From literature [9] it is known, that the saturation concentration of $Mg(OH)_2$ is about 8.9 mg/L (at 18 °C) and that can set a maximum pH of 10.2. From about pH 9, iron can be present in the passive state, resulting in a narrow examination range of pH 9 to about pH 10. This was accomplished by dissolving quantities of 1, 3, 5 and 8 mg/L of solid $Mg(OH)_2$ in distilled water. Due to the electrolyte's susceptibility to lose alkalinity by reacting with CO_2 from ambient air to form $MgCO_3$, the electrolytes were kept under exclusion of air until the measurement was started and the current pH was determined directly before each measurement. Furthermore, defined amounts of NaCl were added to the electrolyte, initially 150, 367 and 584 mg/L. The background for the interaction of chlorides and pH values is a relationship that is well known in the field of corrosion protection of steel in concrete. Here, a [Cl^- to OH^-]-ratio is often used, up to a level where the steel is still expected to be passive. There is a review article from Angst et al. [10] on this subject, in which the authors have found limiting values from 0.09 to 45. Since in the present case

the pH is limited at about 10, additionally even lower NaCl contents of 75, 50 and 25 mg/L were used. Fig. 2 shows the resulting experimental design.

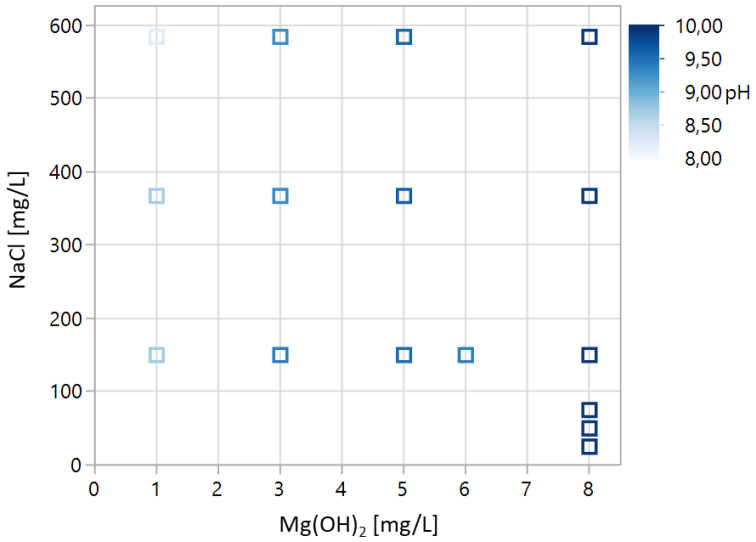

Fig. 2. Experimental design for the determination of the influence of $Mg(OH)_2$ concentration (pH-value) and NaCl concentration on the corrosion behavior of unalloyed steel

To demonstrate the influence of pH (or $Mg(OH)_2$ concentration) in combination with NaCl on the passivity and corrosion of steel in the context of the problem of TiMgN coatings, a special experimental procedure was devised, which takes account to the ongoing mechanisms on this system. For a certain time after contact with the electrolyte, the steel is known to be cathodically protected by the preferred Mg dissolution. To verify this, a pre-polarization of -500 mV_{NHE} of the steel for 10 min was realized immediately after immersing the samples in the test electrolyte. This was followed by another 10-minute period during which the OCP (without external polarization) of the sample was measured. This was followed by an electrochemical impedance spectroscopy measurement (EIS) in the range of 50 kHz to 0.05 Hz, with an amplitude of 10 mV_{RMS} at the last measured OCP. From the EIS measurement, the RP and the electrolyte resistance can be determined (and separated from each other) and thus the corrosion current can be calculated. Further results can be determined from the OCP measurement, e.g. a critical pitting potential (E_{crit}) and the time until it is reached (time to E_{crit}) if localized corrosion or activation has already been initiated within the 10-minute OCP measurement.

3. Results

3.1. OCP´s and corrosion kinetic of TiMgN20 and TiMgN35 on polished and blasted HSS substrates

Fig. 3 shows the curves of measurements on TiMgN with 20 and 35 at-% Mg, respectively on polished and blasted steel. The OCP's mostly start quite negative, but with a tendency to more positive values. The differences between 20 and 35 at% Mg and between polished and corundum blasted substrate are very clear. The same applies to the RP curves, whereby it should be noted here that falling RPs at 20 at-% Mg are due to localized corrosion after about 15 min. For low RPs of <1,000 Ωcm², e.g. at 35 at-% Mg, an enhanced active dissolution of Mg from the TiMgN hard coatings is probably responsible. Higher RPs in the range of 10,000 to > 50,000 Ωcm² indicate almost anodically inert surfaces, from which no or only relatively small amounts of Mg dissolve. For a better summary, the values at 10 minutes (boxed area in Fig. 3) from each of three repeated measurements were used for further statistical evaluation by analysis of variance (ANOVA).

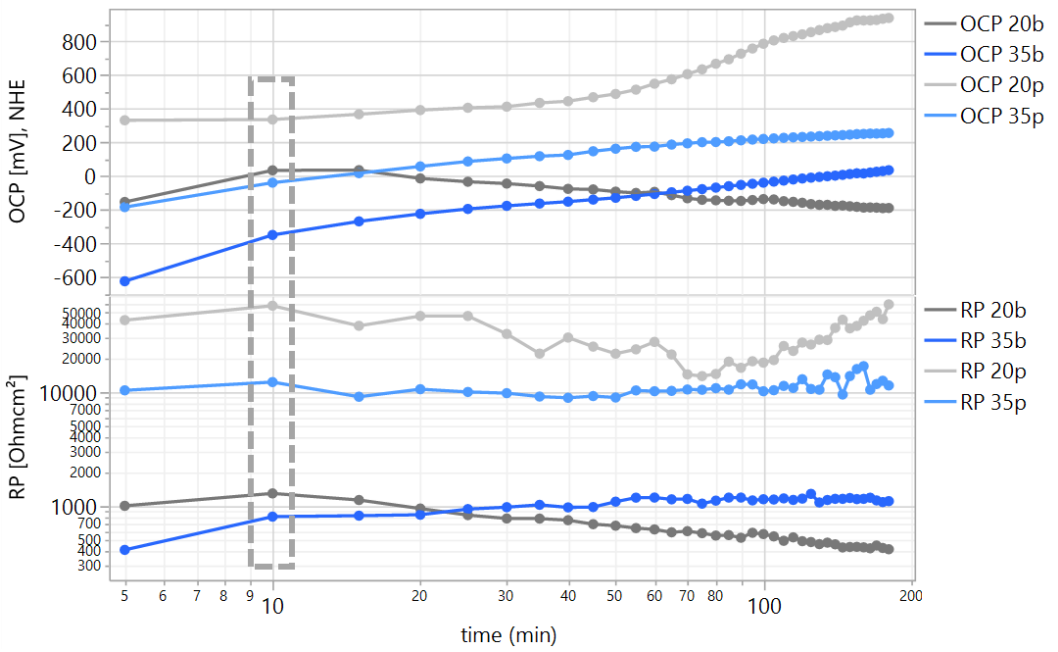

Fig. 3. Example of OCP´s and RP´s over 180 min in 0,8 M NaCl solution, TiMgN with 20 and 35 at-% Mg on corundum blasted (b) and polished (p) HSS, boxed area with values for statistical evaluation

The statistical evaluation (ANOVA) of the values after 10 min indicates a significant influence of the OCP ($r^2 = 0,95$) on the Mg content and surface state and the RP ($r^2 = 0,94$) on the Mg content, surface state and an interaction effect between them. The relationships of the factors are summarized in Fig. 4. For a better assessment of the OCP's, the potential range for actively corroding steel (approx. -350 mV_{NHE}) is shown. After 10 minutes, only samples with 35 at-% Mg on blasted substrate are still well below the potential of active steel. However, since improvements in the corrosion behavior were also observed in other states, it can already be assumed here, that the potential shift cannot be solely responsible for the corrosion protection. In addition, the leaching of magnesium from the TiMgN lattice and the associated changes in the electrolyte at the phase boundary appear to be significant. The strong dependency of the RP's on the Mg content and surface condition already gives an important hint here.

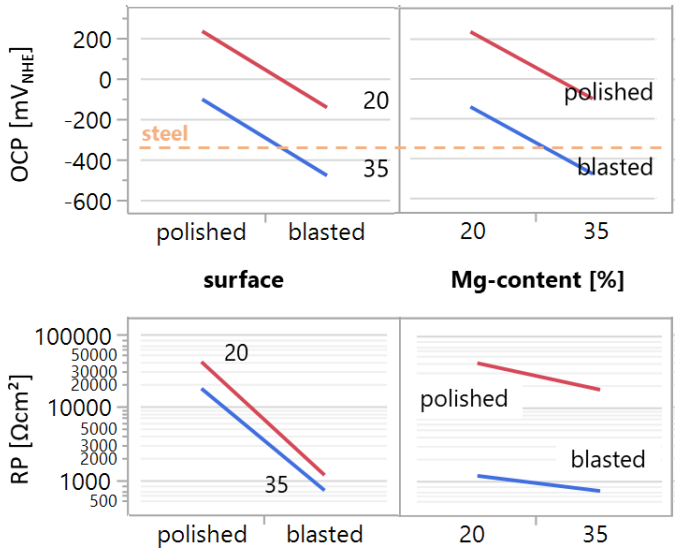

Fig. 4. Factor effects of Mg-content and surface conditions on OCP and RP after 10 min of immersion of TiMgN hard coatings in neutral solutions with different chloride contents, evaluated electrochemical data from Fig. 3 (boxed area)

3.2. Mg dissolution kinetic of TiMgN20 and TiMgN35 on polished and blasted HSS substrates

TiMgN samples with Mg contents of 20 and 35 at-% Mg, both on polished and blasted substrates, were investigated for the released amount of Mg ions by means of a flow cell and ion analysis. Fig. 5 shows the trend of the Mg-ion concentration over an investigation period of 6000 s in a 0.05 M NaCl solution.

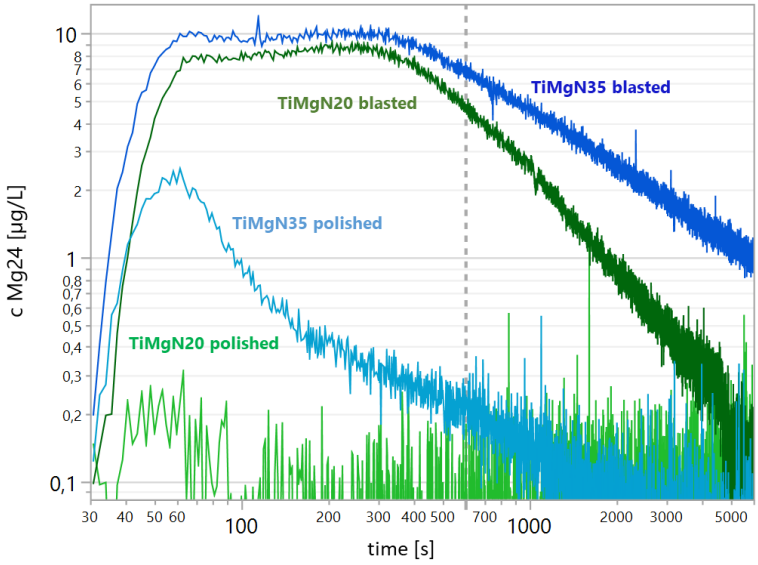

Fig. 5. Instantaneous released Mg ions from TiMgN hard coatings with 20 and 35 at-% Mg content on polished and blasted HSS substrates in 0.05 M NaCl solution using a flow cell with ICP-MS

Already after a very short time of the electrolyte contact, the Mg release increases rapidly. The differences between the Mg contents in combination with the surface state are very clear. TiMgN on corundum blasted substrates and the resulting larger surface release significantly more Mg ions than the polished states. At 35 at-% Mg (polished), a rapid release can be seen at first, but it soon stops again. From the samples with 20 at-% Mg (polished), almost no release of Mg ions is detectable (background noise at 0.2 - 0.3 µg/L). In the corundum blasted state, on the other hand, there is a very long-lasting and strong release. Considering the results from 3.1, this results in a coherent relationship regarding the situation of the OCP's and the RP's. If the release rate of Mg ions is higher, the RP is lower (or the corrosion current is correspondingly higher) and the OCP's tend to be more negative.

3.3. Corrosion behavior of steel in $Mg(OH)_2$ solutions with different NaCl content

The experimental design (Fig. 2) was carried out according to the procedure described in 2.2. After the fixed cathodic polarization at -500 mV_{NHE} for 10 min, the polarization was ceased and the progress of the OCP was followed for another 10 min. As an example, Fig. 6 shows potential curves for three different chloride contents in the case of nearly saturated $Mg(OH)_2$ solution (pH 9.9). In comparison, OCP curves are shown with the same chloride content, but in a pH 7 solution without $Mg(OH)_2$. It can be clearly seen, that in neutral solution with pH 7, corrosion occurs very rapidly within 2-3 min, characterized by the reversal of the potential in the negative direction after an initial rise in the positive direction. The behavior in the $Mg(OH)_2$ solution is different from that. Here, the OCPs increase longer in the positive direction and corrosion occurs only at more positive potentials, whereby the potential drops in the negative direction. The position of the critical potential (E_{crit}) and the time until reaching the critical potential (time to E_{crit}) are used for further evaluation. Following the OCP measurement, an EIS measurement is carried out to determine the RP. Fig. 7 shows the curves for the same three chloride contents in the case of nearly saturated $Mg(OH)_2$ solution (pH 9.9) and in a solution without $Mg(OH)_2$ at pH 7.

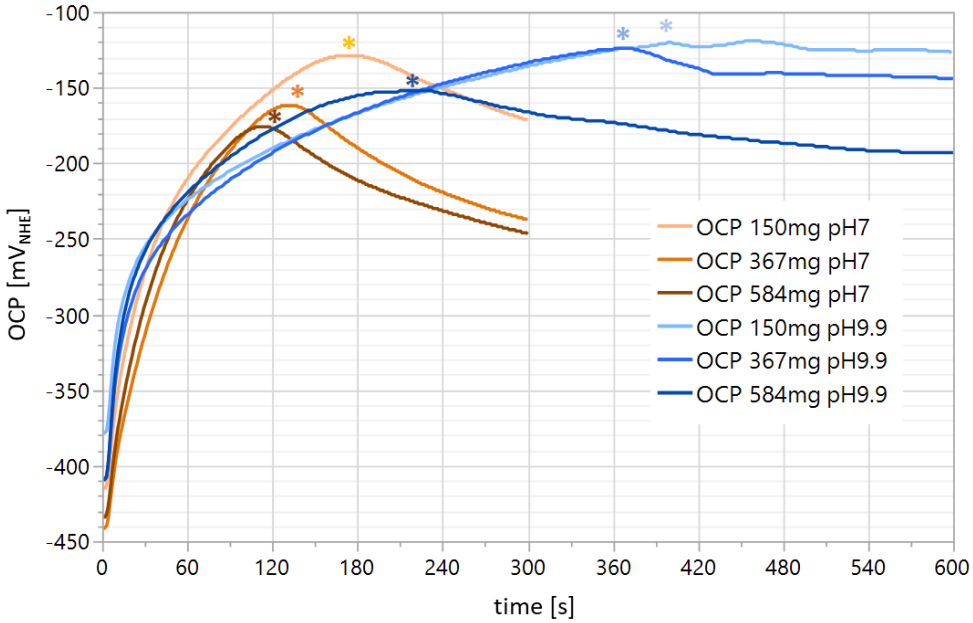

Fig. 6. OCP vs. time plot of C55 unalloyed steel in solutions of $Mg(OH)_2$ (pH 9.9) and neutral water (pH 7) with variation of the NaCl content, "*" indicates E_{crit}

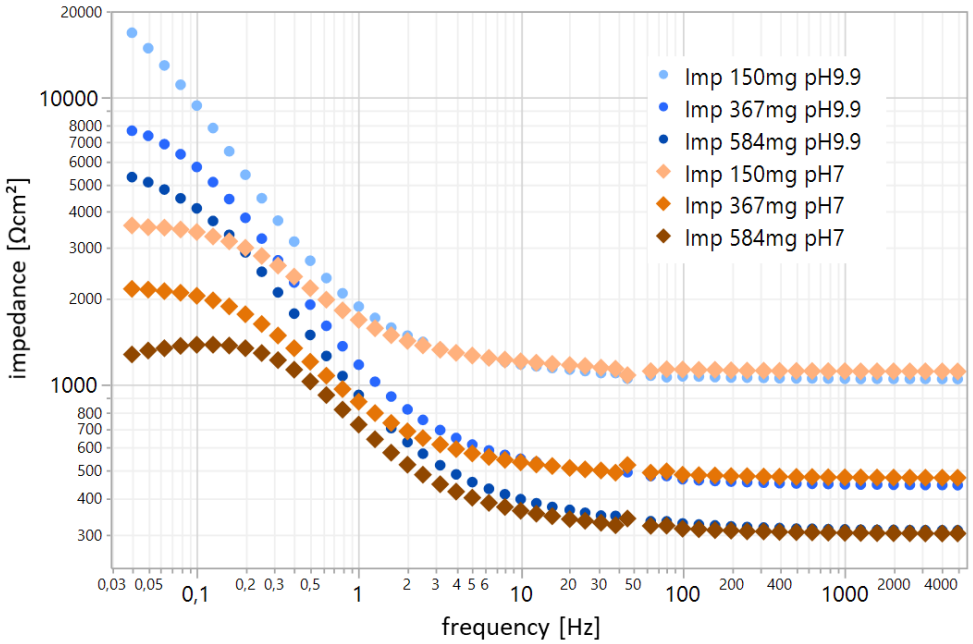

Fig. 7. Impedance vs. frequency plot of C55 unalloyed steel in solutions of $Mg(OH)_2$ (pH 9.9) and neutral water (pH 7) with variation of the NaCl content

For a further statistical evaluation (ANOVA) of the conducted test plan, the corrosion current (i_{corr}) was calculated from the RP. The required B value (i_{corr} = B / RP) was determined by preliminary investigations in analogy to [11]. For steel it is between 0.06 and 0.025 V, depending on the RP. Furthermore, the critical potential and the time until its onset were used for further analysis. For the pH range of 9 to 10, the statistical evaluation showed that E_{crit} primarily depends on the NaCl content (r^2 = 0,74), without significant influence of the pH-value. In contrast, the corrosion current depends on

both the pH and the NaCl content (r^2 = 0,82) and the time to E_{crit} depend on pH, pH*pH and NaCl content (r^2 = 0,80).

Furthermore, the OH^--ion concentration was calculated from the measured pH value and, together with the given chloride ion concentration, the [Cl^- to OH^-] ratio was determined. The results of all investigated electrolyte variants are shown in Fig. 8 as a function of this value, as well as the results of the statistical evaluation of the effects of pH value and NaCl content on i_{corr} and the time to E_{crit}. One can clearly see the effect of alkalization on the relevant electrochemical characteristics. From a [Cl^- to OH^-] ratio of 100 a positive effect starts, below 30 it becomes significant. The corrosion current already decreases by more than a decade at less than a ratio of 30.

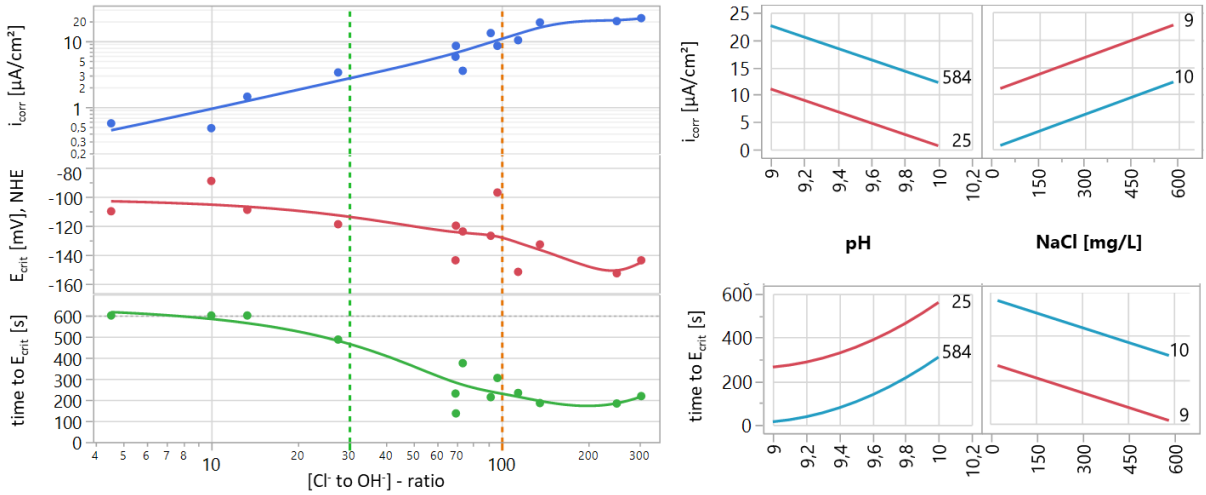

Fig. 8. Influences of pH (due to $Mg(OH)_2$) and NaCl on the corrosion behavior of unalloyed C55 steel, left: electrochemical values vs. [Cl^- to OH^-]-ratio, right: factor effects from ANOVA model

4. Discussion

Electrochemical and analytical data can be used to give a more accurate picture of the corrosion protection mechanisms involved, leading to a significant improvement in the corrosion behavior of TiMgN coatings on steel substrates. The release rate of Mg ions proved to be crucial. With sufficiently high kinetics the potential can be lowered, so that the steel exposed by coating defects is protected cathodically for a short time. The more important and longer-lasting effect is the alkalization of the adjacent electrolyte due to the dissolved Mg ions, which form $Mg(OH)_2$ and allow passivation of steel.

If, for example, the theoretical release of Mg from the first atomic layer (about 0.3 nm) of a model defect of 1 µm diameter at 2.5 µm layer thickness of the TiMgN is calculated, the electrolyte volume of the model defect is enriched by 100-1,000 times that of the solubility for $Mg(OH)_2$, depending on the Mg content of the coatings. As a result, $Mg(OH)_2$ should precipitate out of the electrolyte and strongly buffer it, which in turn prevents the loss of alkalinity, e.g. by reactions of the electrolyte with CO_2 from the ambient air or by formation of magnesium chlorides.

In addition, $Mg(OH)_2$ ensures that no significant hydrolysis reactions occur in conjunction with chlorides, which can also lower the pH, as reported by Lamaka et al. in [12]. Passive steel in alkaline electrolytes in the presence of chloride ions, however, is subject to the risk of localized corrosion, which occurs at a critical pitting potential. However, this potential is much more positive (around 200 mV) than the OCP for general active corrosion, so that the temporary cathodic protection can

extend further in time. The studies on unalloyed steel in the pH range from 9 to 10 showed, that critical chloride contents are to be considered. Significant positive effects are already evident with a [Cl^- to OH^-]-ratio of less than 30. However, since the maximum achievable pH is limited to about 10, only relatively low levels of chloride can thus be effectively tolerated. At a ratio of 30 at pH10 it is 3 mmol/L Cl^-, respectively 289 mg/L NaCl.

However, positive protection effects were also observed under the conditions of the neutral salt spray test (50 g/L NaCl, see Fig. 1). Therefore, another protective effect should be considered which reduces the access of chlorides to the steel via small defects. Since the migration of chlorides always takes place in the direction of the anodic areas, they are temporarily transported to the location of the anodic Mg dissolution and thus away from the steel, which is temporarily cathodically polarized. It can therefore also be assumed that the effective amount of chloride ions at small defects (diameter << coating thickness) is less than the nominal amount in the bulk solution.

5. Conclusions

From the investigations shown here, several responsible mechanisms of corrosion protection in TiMgN hard coatings on steel can be concluded.

- The first mode of action can be explained as a temporary cathodic protection of the low-alloyed steel by the preferred anodic Mg dissolution.
- Related to this is the alkalization of the adjacent electrolyte by formation of $Mg(OH)_2$, which causes the steel to passivate and achieve some tolerance to chloride ions. The relatively large amount of soluble magnesium is likely to cause a buffering effect, which extends the protective effect in time.
- It is also plausible that chloride ions get attracted to the places of the anodic dissolution of Mg from the TiMgN, thus reducing their concentration on the steel substrate.

For different defect types (aspect ratio of diameter to depth or coating thickness), however, a different effective protection can be expected. In large open hole defects, where steel is exposed over a wider area, both the polarization effect and the amount of available $Mg(OH)_2$ are limited, which in addition can lose its alkalinity more quickly by reacting with ambient air (CO_2). By contrast, smaller defects with a high aspect ratio can build up a stable buffered alkaline electrolyte and thus maintain the protection longer.

6. References

[1] M. Fenker, M. Balzer, H. Kappl, O. Banakh: Some properties of (Ti,Mg)N thin films deposited by reactive dc magnetron sputtering, Surf. Coat. Technol. 200 (2005) 227-231
[2] M. Fenker, M. Balzer, H. Kappl, Corrosion behavior of decorative and wear resistant coatings on steel deposited by reactive magnetron sputtering – Tests and improvements, Thin Solid Films 515 (2006) 27-32
[3] Untersuchung des Einflusses von Mg auf das Korrosionsverhalten hartstoffbeschichteter Stahlsubstrate, DFG-funded research project FE 613/3-2 and HE 6160/5-2, 2012 - 2017
[4] Müller, Thoralf; Heyn, Andreas; Balzer, Martin; Fenker, Martin: Untersuchungen zum Einfluss von Magnesium auf das Korrosionsverhalten von TiMgN-Hartstoffschichten auf Stahlsubstraten, Kongress: 15. Sommerkurs Werkstoffe und Fügen (2014), ISBN: 978-3-940961-85-3, S. 187-196 (this article is also available on researchgate.com via authors profiles)

[5] M. Balzer, Identification of the growth defects responsible for pitting corrosion on sputter-coated steel samples by Large Area High Resolution mapping, Thin Solid Films 581 (2015) 99–106
[6] R.W. Bosch, W.F. Bogaerts: Instantaneous Corrosion Rate Measurement with Small-Amplitude Potential Intermodulation Techniques, Corrosion-Vol. 52, No. 3, 204-212, 1996
[7] R.W. Bosch, J. Hubrecht, W.F. Bogaerts, B.C. Syrett: Electrochemical Frequency Modulation: A New Electrochemical Technique for Online Corrosion Monitoring, Corrosion-Vol. 57, No. 1, 60-70, 2001
[8] S.O. Klemm, A.A. Topalov, C.A. Laska, K.J.J. Mayrhofer: Coupling of a high throughput microelectrochemical cell with online multielemental trace analysis by ICP-MS, Electrochemistry Communications 13 (2011), pp. 1533–1535
[9] Weast, R.C. (ed.). Handbook of Chemistry and Physics, 60th ed. Boca Raton, Florida: CRC Press Inc., 1979, p. B-94
[10] U. Angst et al., Critical chloride content in reinforced concrete - A review, Cement and Concrete Research 39 (2009), 1122
[11] M. Babutzka, A. Heyn: Dynamic tafel factor adaption for the evaluation of instantaneous corrosion rates on zinc by using gel-type electrolytes, IOP conference series / Materials science and engineering, Vol. 181.2017, Art. 012021, 12 pages
[12] S. V. Lamaka, R. M. Souto, M. G. S. Ferreira: In-situ visualization of local corrosion by Scanning Ion-selective Electrode Technique (SIET), Microscopy: Science, Technology, Applications and Education, Vol. 3, Formatex Research Center, Badajoz, Spain (2010), p. 2162, available on http://www.formatex.info/microscopy4/2162-2173.pdf.

Acknowledgements

The funding of this work by the German Research Foundation (DFG) under grant no. HE 6160/5-1(2) and FE 613/3-1(2) is gratefully acknowledged!